

Contents lists available at ScienceDirect

Journal of Electrocardiology

journal homepage: www.jecgonline.com

JOURNAL OF Electrocardiology

Prognostic significance of the frontal QRS-T angle in patients with AL cardiac amyloidosis



Anna Turyan Medvedovsky, MD, Arthur Pollak, MD, Mony Shuvy, MD, Israel Gotsman, MD*

Heart Institute, Hadassah University Hospital, Jerusalem, Israel

ARTICLE INFO

Keywords: QRS-T angle Amyloidosis Outcome

ABSTRACT

Introduction: Cardiac involvement is a leading cause of morbidity and mortality in primary light chain (AL) amyloidosis. The electrocardiographic spatial QRS-T angle reflects changes in the direction of the repolarization sequence and is a powerful predictor of outcome in patients with heart failure. We examined the significance of the frontal QRS-T angle in predicting the clinical outcome in patients with AL cardiac amyloidosis.

Methods: Forty-three consecutive patients with cardiac involvement of AL amyloidosis were studied. Patients were followed for survival.

Results: Patient median age was 62 years, 56% were males. After a median follow up of 56 months, 16 out of 43 patients had died (37%). The median QRS-T angle was 102° (interquartile range 35–148). QRS-T angle> 102° was associated with increased prevalence of lambda free light chain disease and the presence of a pleural effusion. It was also associated with increased interventricular septum thickness, smaller left ventricle end-diastolic diameter, echocardiographic myocardial sparkling texture, pericardial effusion, elevated NT-Pro-BNP and increased restrictive physiology evident by increased E/A and E/e`. A QRS-T angle> 102° was a significant predictor of increased mortality by Kaplan-Meier survival analysis ($71.6 \pm 11.1\%$ vs. $45.7 \pm 11.1\%$, P = .02). A QRS-T angle> 102° was an independent predictor of mortality by Cox regression analysis (HR 3.00, 95% CI 1.01–8.89, P < .05).

Conclusions: The QRS-T angle is associated with indices of advanced amyloid disease and is an independent predictor of survival.

© 2020 Elsevier Inc. All rights reserved.

Introduction

Systemic amyloidosis is a relatively rare multisystem disease caused by the deposition of misfolded protein in various tissues leading to organ dysfunction. Primary light chain (AL) amyloidosis, which is the most frequent form, can potentially involve any organ. Cardiac involvement is seen in approximately 50% of these patients and is associated with a poorer prognosis and a more rapid progression of heart failure compared to other types of amyloidosis [1–3]. Amyloid deposition in the heart results in an infiltrative cardiomyopathy, with increased left ventricular (LV) and right ventricular (RV) wall thickness, normal or decreased bi-ventricular cavity size [4]. Early diagnosis of cardiac amyloidosis is critical. Delay in diagnosis may result in patients being unsuitable for the most intensive treatment regimens.

The prognosis of patients with AL amyloidosis varies considerably depending on the nature, number, and extent of organ involvement. Cardiac involvement is a leading cause of morbidity and mortality,

E-mail address: igotsman@bezeqint.net (I. Gotsman).

especially in primary AL amyloidosis [6]. In the past without treatment, the median survival after onset of heart failure was only 6 months [5]. With the development of new strategies, the median survival has increased and treatment can extend life by many years [3].

Prediction of outcome in AL amyloidosis is important for assessment of prognosis and the selection of appropriate therapeutic options. Several laboratory, electrocardiographic, echocardiographic and MRI prognostic factors affect outcome of AL amyloidosis with cardiac involvement. The frontal QRS-T angle, easily obtainable from the surface electrocardiogram (ECG) is an electrocardiographic parameter that reflects changes in the direction of the repolarization sequence and is a marker of electrical instability. Infiltration of the myocardium due to amyloid cardiac involvement should lead to electrical heterogeneities resulting in changes of the repolarization direction and a wider QRS-T angle. The frontal QRS-T angle was a powerful predictor of total mortality and sudden cardiac death in the general population [7]. A wide QRS-T angle was also shown to be a predictor of arrhythmic events in patients with reduced left ventricular function [8,9], reduced survival in chronic heart failure [10] and in myocarditis [11]. There is no data about the prognostic value of the frontal QRS-T angle in patients with AL cardiac amyloidosis. The aim of the present study was to examine

^{*} Corresponding author at: Heart Institute, Hadassah University Hospital, P.O.B 12000, Jerusalem II.-91120. Israel.

the significance of the frontal QRS-T angle in predicting clinical outcome in patients with AL cardiac amyloidosis.

Methods

Forty-three consecutive patients with cardiac involvement of AL amyloidosis followed at the Center for Amyloidosis at Hadassah – Hebrew University Medical Center were studied retrospectively. Patients clinical and laboratory data as well as clinical severity of heart failure and survival data were recorded. For inclusion, at least one biopsy specimen from endomyocardial tissue, bone marrow, rectum, kidney or subcutaneous fat had to be positive for amyloid. The presence for amyloid was visualized by Congo red staining, producing apple-green birefringence under polarized light. Biochemical analyses were performed at the hospital's central laboratory under routine standardized methodologies.

Echocardiograms were performed by a commercially available echocardiographic machine (Vivid Five System, Vingmed-General Electric, Milwaukee, Wisconsin) at the time of diagnosis. Echocardiography data were collected from the institution echocardiography laboratory database. Echocardiography studies including measurements of dimensions were performed according to standard recommendations of the American Society of Echocardiography (ASE) and were evaluated and verified by qualified personnel.

A standard 12-lead electrocardiography was acquired using the MAC 5500 ECG Diagnosis System (Marquette Electronics, Milwaukee, Wisconsin) and were recorded for each patient at diagnosis using standardized procedures. Low QRS voltage was defined as peak QRS amplitudes of <0.5 mV in each limb lead. A pseudo-infarct pattern was defined as Q or QS wave pattern in 2 contiguous leads in the absence of previously documented myocardial infarction. The frontal QRS-T angle was calculated from the frontal QRS and T axis of the baseline 12-lead surface electrocardiogram. It was defined as the absolute value of the difference between the frontal plane QRS axis and T axis and was adjusted to an acute angle by (360°-angle) for an angle larger than 180°.

The institutional committee for human studies of the Hadassah Medical Center approved the study protocol.

SPSS version 17.0 for Windows (SPSS Inc., Chicago, Illinois, USA) was used in all analyses. Continuous variables are presented as median (quartiles), and categorical variables as counts (percentages). Comparison of the clinical characteristics was performed using the Mann-Whitney U test for continuous variables and the Chi-Square Test for categorical variables. Follow-up time was calculated using Kaplan-Meier estimate of potential follow-up. Kaplan-Meier curves, with the logrank test, were used to compare survival, Multivariate Cox proportional hazards regression analysis was used to evaluate independent variables that determined survival. Parameters included in the multivariable analysis were parameters considered clinically important (age and gender) and parameters that were significantly predictive on univariable analysis. The model included age, gender, presence of pleural effusion, electrocardiographic QRS-pseudo-infarction pattern and QRS-T angle>102 using a forward stepwise likelihood ratio selection method. Statistical significance was defined as p < .05.

Results

Baseline clinical characteristics of study population

A total of 43 patients were included in the study. Baseline clinical, laboratory, echocardiographic and electrocardiographic characteristics of the study population are shown in Table 1. The median QRS-T angle was 102° (interquartile range 35–148). Patients were divided based on the median QRST-angle. A wide QRS-T angle (>102°) was associated with increased prevalence of lambda free light chain disease and the presence of a pleural effusion. It was also associated with increased interventricular septum thickness, smaller LV end diastolic diameter,

reduced ejection fraction and pericardial effusion, elevated NT-Pro-BNP and increased restrictive physiology evident by increased echocardiographic mitral inflow E/A ratio and tissue Doppler E/e` ratio.

Predictive value of QRS-T angle for survival

The median follow-up period after the diagnosis of AL amyloidosis was 56 months. During this period 16 out of 43 patients died (37.2%). A QRS-T angle>102° was a significant predictor of increased mortality by Kaplan-Meier survival analysis (71.6 \pm 11.1% vs. 45.7 \pm 11.1%, P = .02), Fig. 1. Univariable cox regression analyses of clinical predictors of mortality are presented in Table 2. Multivariable Cox regression analysis after adjustment for clinically relevant parameters demonstrated that a wide QRS-T angle>102° was an independent predictor of increased mortality (hazard ratio 3.00, 95% confidence interval 1.01–8.89, P = .04). The electrocardiographic pseudo-infarction pattern was also an independent predictor of mortality (hazard ratio 4.94, 95% confidence interval 1.39–17.6, P = .01).

Discussion

In the present study we evaluated the relation between the frontal QRS-T angle and outcome in patients with AL cardiac amyloidosis followed in a tertiary referral center for the treatment of cardiac amyloidosis. The main result of the study is that the frontal QRS-T angle is a powerful prognostic marker in risk assessment of patients with AL amyloidosis and cardiac involvement.

The QRS-T angle, the angle between the directions of ventricular electrical depolarization and repolarization, represents abnormal cardiac structure and electrical heterogeneities resulting in changes of the repolarization direction. A wide QRS-T angle has been shown to be a marker of electrical instability [7] in the general population, was a strong predictor of arrhythmic events in patients with reduced left ventricular function [8,9] and conveys a poor prognosis in patients with HF [10]. The QRS-T angle was directly associated with reduction of LV systolic function [12] and widening of the QRS-T angle overtime has been shown to be associated with deterioration of the LV systolic function [8] as well as with reduced survival in patients with heart failure [12].

The QRS-T angle has not been analyzed before in patients with amyloidosis. In the present study we found that the median frontal QRS-T angle in patient with cardiac amyloidosis was 102°. A wide ORS-T angle (>102°) was associated with indices of advanced amyloid myocardial involvement and was an independent predictor of increased mortality in patients with AL cardiac amyloidosis. The wide QRS-T angle in our study was associated with indices of more advanced cardiac amyloid disease: increased LV wall thickness with smaller dimensions, LV diastolic dysfunction and systolic dysfunction. The more advanced disease with increased infiltration of the myocardium would cause electrical heterogeneities resulting in changes of the repolarization direction and a wider QRS-T angle. Given the significant impact of cardiac involvement on clinical outcome in cardiac amyloidosis [3] and the association of the QRS-T angle with structural damage to the myocardium, as seen in this study as well as previous studies, it is likely that the QRS-T angle is associated with a poor prognosis. A wide QRS-T angle represents more advanced myocardial disease and would convey prognostic significant in patients with cardiac amyloidosis.

While there are numerous parameters that convey prognostic importance in patients with AL amyloidosis with cardiac evolvement including biomarkers, echocardiographic and MRI features, the ECG is a standard and readily available parameter that can help convey important prognostic information in these patients. As shown in the present study, the QRS-T angle is associated with more advanced cardiac involvement and more importantly, with prognostic information. We believe that the ECG can help in assessing outcome in patients with AL amyloidosis.

 Table 1

 Clinical, electrocardiographic and echocardiographic characteristics of the study population stratified according to the frontal QRS-T angle.

Clinical characteristics	QRS-T angle $\leq 102^{\circ}$ ($N = 22$)	QRS-T angle $> 102^{\circ}$ ($N = 21$)	All (N = 43)	P value
Age at Diagnosis (years)	64 (52-65)	61 (54-66)	62 (52-65)	0.93
Gender (male)	14 (64)	10 (48)	24 (56)	0.29
NYHA class III/IV	19 (86)	17 (81)	36 (84)	0.63
Mayo Clinic Prognostic Stage 3-4	14 (64)	17 (85)	31 (74)	0.12
Symptoms Duration (Days)	165 (120-270)	210 (90-435)	180 (120-360)	0.68
Atrial Fibrillation	2 (9)	4 (19)	6 (14)	0.35
Pleural Effusion	6 (27)	14 (67)	20 (47)	0.01
Non-cardiac organs involved:	- (=-)	(,	()	
Renal	9 (41)	6 (29)	15 (35)	0.4
Hepatic/Gastrointestinal	10 (45)	9 (43)	19 (44)	0.86
Lung	0 (0)	2 (10)	2 (5)	0.14
Neuropathic	5 (23)	5 (24)	10 (23)	0.93
Soft tissue bone	8 (36)		12 (28)	0.33
		4 (19)	, ,	
Body mass index (kg/m²)	26 (22–27)	24 (21–29)	25 (22–28)	0.48
Systolic BP (mmHg)	106 (92–119)	111 (95–116)	106 (95–116)	0.79
Diastolic BP (mmHg)	65 (60–74)	67 (61–75)	66 (60–74)	0.59
Heart rate (beats/min)	81 (76–85)	84 (74–98)	82 (76–94)	0.34
Diuretics (%)	19 (86)	19 (90)	38 (88)	0.67
Angiotensin converting enzyme inhibitor (%)	6 (27)	4 (19)	10 (23)	0.52
Beta blockers (%)	8 (36)	6 (29)	14 (33)	0.59
Biomarkers				
Hs-Troponin-I (ng/mL)	0.1 (0.0-0.2)	0.1 (0.0-0.2)	0.1 (0.0-0.2)	0.75
NT-pro-BNP (pg/mL)	2175	4591	4373	0.23
1 (10)	(1066-6822)	(2496-7014)	(1500-6756)	
Free kappa light chain (mg/L)	50 (16-678)	12 (6.9–24)	23 (9.1–346)	0.01
Free lambda light chain (mg/L)	34 (11-332)	250 (64-528)	146 (14-442)	0.05
Kappa/lambda ratio	1.8 (0.1-47)	0.0 (0.0-0.2)	0.2 (0.0-14)	0.01
FLC lambda Type (%)	11 (50)	17 (81)	28 (65)	0.03
FLC difference (mg/L)	434 (63-809)	264 (138–588)	337 (123-706)	0.50
Albumin (mg/L)	39 (35–41)	35 (32–42)	37 (33–41)	0.48
	QRS-T angle ≤ 102°	QRS-T angle > 102°	All	
Electrocardiographic characteristics	(N = 22)	(N = 21)	(N = 43)	P value
Heart rate (beats per minute)	78 (64–85)	84 (72–97)	81 (71-89)	0.11
	164 (150-190)	172 (153-185)	168 (152-190)	0.96
PR interval (ms)				
PR interval (ms) QRS interval (ms)	95 (84–103)	92 (83–107)	94 (84–104)	0.96
QRS interval (ms)	95 (84–103)	, ,	, ,	
QRS interval (ms) Corrected QT interval (ms)	95 (84–103) 468 (448–490)	472 (443–483)	472 (448–486)	0.90
QRS interval (ms) Corrected QT interval (ms) P axis (°)	95 (84–103) 468 (448–490) 52 (34–65)	472 (443–483) 44 (29–56)	472 (448–486) 47 (29–65)	0.90 0.44
QRS interval (ms) Corrected QT interval (ms) P axis (°) QRS axis (°)	95 (84–103) 468 (448–490) 52 (34–65) 25 (–19.5–92)	472 (443–483) 44 (29–56) 9.0 (–53.5–215)	472 (448–486) 47 (29–65) 18 (–40.0–151)	0.90 0.44 0.78
QRS interval (ms) Corrected QT interval (ms) P axis (°) QRS axis (°) T axis (°)	95 (84–103) 468 (448–490) 52 (34–65) 25 (-19.5–92) 46 (5.5–83)	472 (443–483) 44 (29–56) 9.0 (–53.5–215) 85 (53–138)	472 (448–486) 47 (29–65) 18 (–40.0–151) 66 (32–119)	0.90 0.44 0.78 0.01
QRS interval (ms) Corrected QT interval (ms) P axis (°) QRS axis (°) T axis (°) QRS-T angle (°)	95 (84–103) 468 (448–490) 52 (34–65) 25 (-19.5–92) 46 (5.5–83) 36 (16–70)	472 (443–483) 44 (29–56) 9.0 (–53.5–215) 85 (53–138) 148 (120–159)	472 (448–486) 47 (29–65) 18 (–40.0–151) 66 (32–119) 102 (35–148)	0.90 0.44 0.78 0.01 <0.001
QRS interval (ms) Corrected QT interval (ms) P axis (°) QRS axis (°) T axis (°) QRS-T angle (°) Low QRS voltage	95 (84–103) 468 (448–490) 52 (34–65) 25 (-19.5–92) 46 (5.5–83) 36 (16–70) 17 (77)	472 (443–483) 44 (29–56) 9.0 (–53.5–215) 85 (53–138) 148 (120–159) 19 (90)	472 (448–486) 47 (29–65) 18 (-40.0–151) 66 (32–119) 102 (35–148) 36 (84)	0.90 0.44 0.78 0.01 <0.001 0.24
QRS interval (ms) Corrected QT interval (ms) P axis (°) QRS axis (°) T axis (°) QRS-T angle (°) Low QRS voltage Pseudo infarction pattern	95 (84–103) 468 (448–490) 52 (34–65) 25 (-19.5–92) 46 (5.5–83) 36 (16–70) 17 (77) 10 (45)	472 (443–483) 44 (29–56) 9.0 (–53.5–215) 85 (53–138) 148 (120–159) 19 (90) 14 (67)	472 (448–486) 47 (29–65) 18 (–40.0–151) 66 (32–119) 102 (35–148) 36 (84) 24 (56)	0.90 0.44 0.78 0.01 <0.001 0.24
* *	95 (84–103) 468 (448–490) 52 (34–65) 25 (-19.5–92) 46 (5.5–83) 36 (16–70) 17 (77) 10 (45) 3 (14)	472 (443–483) 44 (29–56) 9.0 (–53.5–215) 85 (53–138) 148 (120–159) 19 (90) 14 (67) 2 (10)	472 (448–486) 47 (29–65) 18 (–40.0–151) 66 (32–119) 102 (35–148) 36 (84) 24 (56) 5 (12)	0.90 0.44 0.78 0.01 <0.001 0.24
QRS interval (ms) Corrected QT interval (ms) P axis (°) QRS axis (°) T axis (°) QRS-T angle (°) Low QRS voltage Pseudo infarction pattern I/II degree atrioventricular block Left/Right Bundle Branch block	95 (84–103) 468 (448–490) 52 (34–65) 25 (-19.5–92) 46 (5.5–83) 36 (16–70) 17 (77) 10 (45)	472 (443–483) 44 (29–56) 9.0 (–53.5–215) 85 (53–138) 148 (120–159) 19 (90) 14 (67)	472 (448–486) 47 (29–65) 18 (–40.0–151) 66 (32–119) 102 (35–148) 36 (84) 24 (56)	0.90 0.44 0.78 0.01 <0.001 0.24 0.16 0.67
QRS interval (ms) Corrected QT interval (ms) P axis (°) QRS axis (°) T axis (°) QRS-T angle (°) Low QRS voltage Pseudo infarction pattern I/II degree atrioventricular block Left/Right Bundle Branch block Echocardiographic characteristics	95 (84–103) 468 (448–490) 52 (34–65) 25 (-19.5–92) 46 (5.5–83) 36 (16–70) 17 (77) 10 (45) 3 (14) 7 (32)	472 (443-483) 44 (29-56) 9.0 (-53.5-215) 85 (53-138) 148 (120-159) 19 (90) 14 (67) 2 (10) 3 (14)	472 (448-486) 47 (29-65) 18 (-40.0-151) 66 (32-119) 102 (35-148) 36 (84) 24 (56) 5 (12) 10 (23)	0.90 0.44 0.78 0.01 <0.001 0.24 0.16 0.67 0.17
QRS interval (ms) Corrected QT interval (ms) P axis (°) QRS axis (°) T axis (°) QRS-T angle (°) Low QRS voltage Pseudo infarction pattern I/II degree atrioventricular block Left/Right Bundle Branch block Echocardiographic characteristics LV end-diastolic diameter (mm)	95 (84–103) 468 (448–490) 52 (34–65) 25 (-19.5–92) 46 (5.5–83) 36 (16–70) 17 (77) 10 (45) 3 (14) 7 (32)	472 (443-483) 44 (29-56) 9.0 (-53.5-215) 85 (53-138) 148 (120-159) 19 (90) 14 (67) 2 (10) 3 (14) 43 (38-47)	472 (448-486) 47 (29-65) 18 (-40.0-151) 66 (32-119) 102 (35-148) 36 (84) 24 (56) 5 (12) 10 (23)	0.90 0.44 0.78 0.01 <0.001 0.24 0.16 0.67 0.17
QRS interval (ms) Corrected QT interval (ms) P axis (°) QRS axis (°) T axis (°) QRS-T angle (°) Low QRS voltage Pseudo infarction pattern I/II degree atrioventricular block Left/Right Bundle Branch block Echocardiographic characteristics LV end-diastolic diameter (mm) LV end-systolic diameter (mm)	95 (84–103) 468 (448–490) 52 (34–65) 25 (-19.5–92) 46 (5.5–83) 36 (16–70) 17 (77) 10 (45) 3 (14) 7 (32) 47 (44–49) 30 (27–33)	472 (443-483) 44 (29-56) 9.0 (-53.5-215) 85 (53-138) 148 (120-159) 19 (90) 14 (67) 2 (10) 3 (14) 43 (38-47) 29 (26-34)	472 (448–486) 47 (29–65) 18 (-40.0–151) 66 (32–119) 102 (35–148) 36 (84) 24 (56) 5 (12) 10 (23) 46 (40–49) 30 (26–33)	0.90 0.44 0.78 0.01 <0.001 0.24 0.16 0.67 0.17
QRS interval (ms) Corrected QT interval (ms) P axis (°) QRS axis (°) I axis (°) QRS-T angle (°) Low QRS voltage Pseudo infarction pattern I/II degree atrioventricular block Left/Right Bundle Branch block Echocardiographic characteristics LV end-diastolic diameter (mm) LV end-systolic diameter (mm) IVS thickness (mm)	95 (84–103) 468 (448–490) 52 (34–65) 25 (-19.5–92) 46 (5.5–83) 36 (16–70) 17 (77) 10 (45) 3 (14) 7 (32) 47 (44–49) 30 (27–33) 13 (11–14)	472 (443-483) 44 (29-56) 9.0 (-53.5-215) 85 (53-138) 148 (120-159) 19 (90) 14 (67) 2 (10) 3 (14) 43 (38-47) 29 (26-34) 14 (13-15)	472 (448–486) 47 (29–65) 18 (-40.0–151) 66 (32–119) 102 (35–148) 36 (84) 24 (56) 5 (12) 10 (23) 46 (40–49) 30 (26–33) 14 (12–15)	0.90 0.44 0.78 0.01 <0.001 0.24 0.16 0.67 0.17
QRS interval (ms) Corrected QT interval (ms) P axis (°) QRS axis (°) QRS axis (°) QRS-T angle (°) Low QRS voltage Pseudo infarction pattern I/II degree atrioventricular block Left/Right Bundle Branch block Echocardiographic characteristics LV end-diastolic diameter (mm) LV end-systolic diameter (mm) LV posterior wall thickness (mm) LV posterior wall thickness (mm)	95 (84-103) 468 (448-490) 52 (34-65) 25 (-19.5-92) 46 (5.5-83) 36 (16-70) 17 (77) 10 (45) 3 (14) 7 (32) 47 (44-49) 30 (27-33) 13 (11-14) 12 (10-14)	472 (443-483) 44 (29-56) 9.0 (-53,5-215) 85 (53-138) 148 (120-159) 19 (90) 14 (67) 2 (10) 3 (14) 43 (38-47) 29 (26-34) 14 (13-15) 13 (12-14)	472 (448–486) 47 (29–65) 18 (-40.0–151) 66 (32–119) 102 (35–148) 36 (84) 24 (56) 5 (12) 10 (23) 46 (40–49) 30 (26–33) 14 (12–15) 13 (11–14)	0.90 0.44 0.78 0.01 <0.001 0.24 0.16 0.67 0.17
QRS interval (ms) Corrected QT interval (ms) P axis (°) QRS axis (°) T axis (°) QRS-T angle (°) Low QRS voltage Pseudo infarction pattern I/II degree atrioventricular block Left/Right Bundle Branch block Echocardiographic characteristics LV end-diastolic diameter (mm) LV end-systolic diameter (mm) LV posterior wall thickness (mm) LV posterior wall thickness (mm) LV Ejection fraction (%)	95 (84-103) 468 (448-490) 52 (34-65) 25 (-19.5-92) 46 (5.5-83) 36 (16-70) 17 (77) 10 (45) 3 (14) 7 (32) 47 (44-49) 30 (27-33) 13 (11-14) 12 (10-14) 55 (41-60)	472 (443-483) 44 (29-56) 9.0 (-53.5-215) 85 (53-138) 148 (120-159) 19 (90) 14 (67) 2 (10) 3 (14) 43 (38-47) 29 (26-34) 14 (13-15) 13 (12-14) 43 (40-48)	472 (448-486) 47 (29-65) 18 (-40.0-151) 66 (32-119) 102 (35-148) 36 (84) 24 (56) 5 (12) 10 (23) 46 (40-49) 30 (26-33) 14 (12-15) 13 (11-14) 45 (40-60)	0.90 0.44 0.78 0.01 <0.001 0.24 0.16 0.67 0.17 0.04 0.50 0.04 0.07
QRS interval (ms) Corrected QT interval (ms) P axis (*) QRS axis (*) QRS axis (*) QRS-T angle (*) Low QRS voltage Pseudo infarction pattern I/II degree atrioventricular block Left/Right Bundle Branch block Echocardiographic characteristics LV end-diastolic diameter (mm) LV end-systolic diameter (mm) LV posterior wall thickness (mm) LV Ejection fraction (*) LV Ejection fraction (50%)	95 (84–103) 468 (448–490) 52 (34–65) 25 (-19.5–92) 46 (5.5–83) 36 (16–70) 17 (77) 10 (45) 3 (14) 7 (32) 47 (44–49) 30 (27–33) 13 (11–14) 12 (10–14) 55 (41–60) 10 (45)	472 (443-483) 44 (29-56) 9.0 (-53.5-215) 85 (53-138) 148 (120-159) 19 (90) 14 (67) 2 (10) 3 (14) 43 (38-47) 29 (26-34) 14 (13-15) 13 (12-14) 43 (40-48) 16 (76)	472 (448-486) 47 (29-65) 18 (-40.0-151) 66 (32-119) 102 (35-148) 36 (84) 24 (56) 5 (12) 10 (23) 46 (40-49) 30 (26-33) 14 (12-15) 13 (11-14) 45 (40-60) 26 (60)	0.90 0.44 0.78 0.01 <0.001 0.24 0.16 0.67 0.17 0.04 0.50 0.04 0.07 0.09 0.04
QRS interval (ms) Corrected QT interval (ms) P axis (°) QRS axis (°) T axis (°) QRS-T angle (°) Low QRS voltage Pseudo infarction pattern I/II degree atrioventricular block Left/Right Bundle Branch block Echocardiographic characteristics LV end-diastolic diameter (mm) LV end-systolic diameter (mm) IVS thickness (mm) LV posterior wall thickness (mm) LV Ejection fraction (%) LV Ejection fraction <50% Myocardial granular sparkling texture	95 (84–103) 468 (448–490) 52 (34–65) 25 (-19.5–92) 46 (5.5–83) 36 (16–70) 17 (77) 10 (45) 3 (14) 7 (32) 47 (44–49) 30 (27–33) 13 (11–14) 12 (10–14) 55 (41–60) 10 (45) 12 (63)	472 (443-483) 44 (29-56) 9.0 (-53.5-215) 85 (53-138) 148 (120-159) 19 (90) 14 (67) 2 (10) 3 (14) 43 (38-47) 29 (26-34) 14 (13-15) 13 (12-14) 43 (40-48) 16 (76) 15 (94)	472 (448-486) 47 (29-65) 18 (-40.0-151) 66 (32-119) 102 (35-148) 36 (84) 24 (56) 5 (12) 10 (23) 46 (40-49) 30 (26-33) 14 (12-15) 13 (11-14) 45 (40-60) 26 (60) 27 (77)	0.90 0.44 0.78 0.01 <0.001 0.24 0.16 0.67 0.17 0.04 0.50 0.04 0.07 0.09 0.04
QRS interval (ms) Corrected QT interval (ms) P axis (°) QRS axis (°) QRS axis (°) QRS-T angle (°) Low QRS voltage Pseudo infarction pattern I/II degree atrioventricular block Left/Right Bundle Branch block Echocardiographic characteristics LV end-diastolic diameter (mm) LV end-systolic diameter (mm) LV posterior wall thickness (mm) LV posterior wall thickness (mm) LV Ejection fraction (%) LV Ejection fraction <50% Myocardial granular sparkling texture LA diameter (mm)	95 (84–103) 468 (448–490) 52 (34–65) 25 (-19.5–92) 46 (5.5–83) 36 (16–70) 17 (77) 10 (45) 3 (14) 7 (32) 47 (44–49) 30 (27–33) 13 (11–14) 12 (10–14) 55 (41–60) 10 (45) 12 (63) 44 (41–48)	472 (443-483) 44 (29-56) 9.0 (-53.5-215) 85 (53-138) 148 (120-159) 19 (90) 14 (67) 2 (10) 3 (14) 43 (38-47) 29 (26-34) 14 (13-15) 13 (12-14) 43 (40-48) 16 (76) 15 (94) 43 (38-50)	472 (448-486) 47 (29-65) 18 (-40.0-151) 66 (32-119) 102 (35-148) 36 (84) 24 (56) 5 (12) 10 (23) 46 (40-49) 30 (26-33) 14 (12-15) 13 (11-14) 45 (40-60) 26 (60) 27 (77) 43 (40-48)	0.90 0.44 0.78 0.01 <0.001 0.24 0.16 0.67 0.17 0.04 0.50 0.04 0.07 0.09 0.04 0.03
QRS interval (ms) Corrected QT interval (ms) P axis (°) QRS axis (°) QRS axis (°) QRS-T angle (°) Low QRS voltage Pseudo infarction pattern I/Il degree atrioventricular block Left/Right Bundle Branch block Echocardiographic characteristics LV end-diastolic diameter (mm) LV end-systolic diameter (mm) IVS thickness (mm) LV posterior wall thickness (mm) LV Ejection fraction (%) LV Ejection fraction <50% Myocardial granular sparkling texture LA diameter (mm) TR gradient (mmHg)	95 (84–103) 468 (448–490) 52 (34–65) 25 (-19.5–92) 46 (5.5–83) 36 (16–70) 17 (77) 10 (45) 3 (14) 7 (32) 47 (44–49) 30 (27–33) 13 (11–14) 12 (10–14) 55 (41–60) 10 (45) 12 (63)	472 (443-483) 44 (29-56) 9.0 (-53.5-215) 85 (53-138) 148 (120-159) 19 (90) 14 (67) 2 (10) 3 (14) 43 (38-47) 29 (26-34) 14 (13-15) 13 (12-14) 43 (40-48) 16 (76) 15 (94)	472 (448-486) 47 (29-65) 18 (-40.0-151) 66 (32-119) 102 (35-148) 36 (84) 24 (56) 5 (12) 10 (23) 46 (40-49) 30 (26-33) 14 (12-15) 13 (11-14) 45 (40-60) 26 (60) 27 (77)	0.90 0.44 0.78 0.01 <0.001 0.24 0.16 0.67 0.17 0.04 0.50 0.04 0.07 0.09 0.04 0.03
QRS interval (ms) Corrected QT interval (ms) P axis (°) QRS axis (°) QRS axis (°) QRS-T angle (°) Low QRS voltage Pseudo infarction pattern I/Il degree atrioventricular block Left/Right Bundle Branch block Echocardiographic characteristics LV end-diastolic diameter (mm) LV end-systolic diameter (mm) IVS thickness (mm) LV posterior wall thickness (mm) LV Ejection fraction (%) LV Ejection fraction <50% Myocardial granular sparkling texture LA diameter (mm) TR gradient (mmHg)	95 (84–103) 468 (448–490) 52 (34–65) 25 (-19.5–92) 46 (5.5–83) 36 (16–70) 17 (77) 10 (45) 3 (14) 7 (32) 47 (44–49) 30 (27–33) 13 (11–14) 12 (10–14) 55 (41–60) 10 (45) 12 (63) 44 (41–48)	472 (443-483) 44 (29-56) 9.0 (-53.5-215) 85 (53-138) 148 (120-159) 19 (90) 14 (67) 2 (10) 3 (14) 43 (38-47) 29 (26-34) 14 (13-15) 13 (12-14) 43 (40-48) 16 (76) 15 (94) 43 (38-50)	472 (448-486) 47 (29-65) 18 (-40.0-151) 66 (32-119) 102 (35-148) 36 (84) 24 (56) 5 (12) 10 (23) 46 (40-49) 30 (26-33) 14 (12-15) 13 (11-14) 45 (40-60) 26 (60) 27 (77) 43 (40-48)	0.90 0.44 0.78 0.01 <0.001 0.24 0.16 0.67 0.17 0.04 0.50 0.04 0.07 0.09 0.04 0.03 0.93
QRS interval (ms) Corrected QT interval (ms) P axis (°) QRS axis (°) T axis (°) QRS-T angle (°) Low QRS voltage Pseudo infarction pattern I/II degree atrioventricular block Left/Right Bundle Branch block Echocardiographic characteristics LV end-diastolic diameter (mm) LV end-systolic diameter (mm) IVS thickness (mm) LV posterior wall thickness (mm) LV Ejection fraction (%) LV Ejection fraction <50% Myocardial granular sparkling texture LA diameter (mm) TR gradient (mmHg) Pericardial effusion	95 (84-103) 468 (448-490) 52 (34-65) 25 (-19.5-92) 46 (5.5-83) 36 (16-70) 17 (77) 10 (45) 3 (14) 7 (32) 47 (44-49) 30 (27-33) 13 (11-14) 12 (10-14) 55 (41-60) 10 (45) 12 (63) 44 (41-48) 27 (24-36)	472 (443-483) 44 (29-56) 9.0 (-53.5-215) 85 (53-138) 148 (120-159) 19 (90) 14 (67) 2 (10) 3 (14) 43 (38-47) 29 (26-34) 14 (13-15) 13 (12-14) 43 (40-48) 16 (76) 15 (94) 43 (38-50) 26 (22-35)	472 (448-486) 47 (29-65) 18 (-40.0-151) 66 (32-119) 102 (35-148) 36 (84) 24 (56) 5 (12) 10 (23) 46 (40-49) 30 (26-33) 14 (12-15) 13 (11-14) 45 (40-60) 26 (60) 27 (77) 43 (40-48) 27 (23-35)	0.90 0.44 0.78 0.01 <0.001 0.24 0.16 0.67 0.17 0.04 0.50 0.04 0.07 0.09 0.04 0.03 0.93 0.67
QRS interval (ms) Corrected QT interval (ms) P axis (°) QRS axis (°) T axis (°) QRS-T angle (°) Low QRS voltage Pseudo infarction pattern I/II degree atrioventricular block Left/Right Bundle Branch block	95 (84-103) 468 (448-490) 52 (34-65) 25 (-19.5-92) 46 (5.5-83) 36 (16-70) 17 (77) 10 (45) 3 (14) 7 (32) 47 (44-49) 30 (27-33) 13 (11-14) 12 (10-14) 55 (41-60) 10 (45) 12 (63) 44 (41-48) 27 (24-36) 8 (40)	472 (443-483) 44 (29-56) 9.0 (-53.5-215) 85 (53-138) 148 (120-159) 19 (90) 14 (67) 2 (10) 3 (14) 43 (38-47) 29 (26-34) 14 (13-15) 13 (12-14) 43 (40-48) 16 (76) 15 (94) 43 (38-50) 26 (22-35) 13 (65)	472 (448-486) 47 (29-65) 18 (-40.0-151) 66 (32-119) 102 (35-148) 36 (84) 24 (56) 5 (12) 10 (23) 46 (40-49) 30 (26-33) 14 (12-15) 13 (11-14) 45 (40-60) 26 (60) 27 (77) 43 (40-48) 27 (23-35) 21 (53)	0.90 0.44 0.78 0.01 <0.001 0.24 0.16 0.67 0.17 0.04 0.50 0.04 0.07 0.09 0.04 0.03 0.93 0.67 0.11

Data is presented as median (inter-quartile range) for continuous variables and counts (percentages) for categorical variables. P value by the Mann-Whitney U test for continuous variables and the Chi-Square Test for categorical variables.

CA: cardiac amyloidosis. BMI: body mass index; NYHA class: New York Heart Association functional classification; pro-BNP: N-terminal pro-B-type natriuretic peptide; LV: left ventricle; RV: right ventricle; LA: left atrium; IVS: interventricular septum; LVMI: left mass indexed to body surface area; E: early diastolic peak filling velocity; A: late diastolic peak filling velocity, E': tissue Doppler early diastolic septal mitral annular velocity.

Mayo Clinic Prognostic Stage was calculated using the revised Mayo Clinic prognostic staging system for light chain amyloidosis based on NT-pro-BNP, cardiac troponin T and serum free light chains [13].

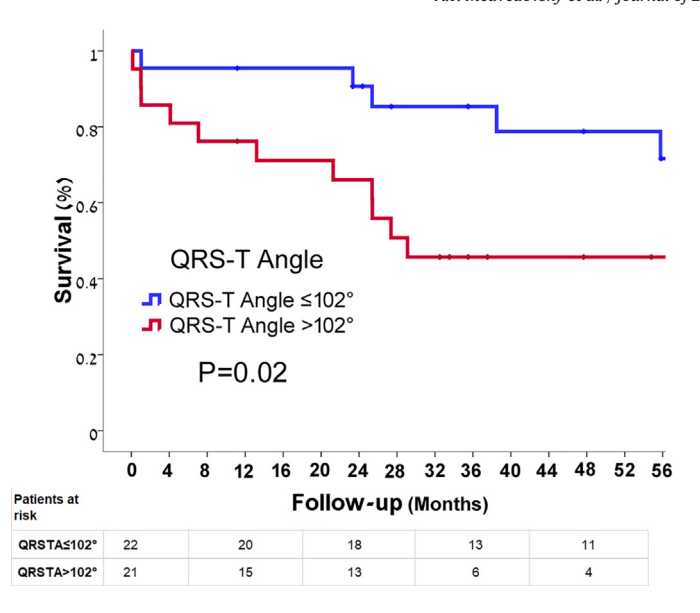


Fig. 1. Overall survival in patients with AL amyloidosis Survival of patients with AL amyloidosis represented by Kaplan-Meier survival curves. according to QRS-T angle. A QRS-T angle>102° was a significant predictor of increased. mortality (71.6 \pm 11.1% vs. 45.7 \pm 11.1%, P=.02).

Table 2Clinical Predictors of mortality by Cox regression analysis.

Variable	Univariable		
	Hazard ratio (95% CI)	P value	
Age (>62 years)	0.73 (0.27-1.96)	0.53	
Male Gender	1.76 (0.64-4.87)	0.28	
NYHA class III/IV	4.41 (0.58-33.76)	0.15	
Pleural Effusion	3.69 (1.26-10.79)	0.02	
Hs-Troponin-I (>0.025 ng/mL)	1.60 (0.36-7.06)	0.54	
NT-pro-BNP (>1800 pg/mL)	3.14 (0.71-13.93)	0.13	
FLC difference (>180 mg/L)	1.43 (0.46-4.45)	0.54	
Mayo Prognostic Stage 3-4	3.21 (0.73-14.18)	0.12	
Free Kappa LC (>23 mg/L)	0.48 (0.17-1.34)	0.16	
Free lambda LC (>130 mg/L)	1.41 (0.52-3.79)	0.50	
Kappa/lambda ratio (>0.15)	0.42 (0.15-1.17)	0.10	
Low QRS voltage	0.43 (0.15-1.25)	0.12	
Pseudo-infarction pattern	5.18 (1.46-18.34)	0.01	
QRST-A > 102°	3.20 (1.10-9.32)	0.03	
Myocardial granular sparkling texture	3.75 (0.49-28.91)	0.20	
Pericardial Effusion	1.93 (0.64-5.75)	0.24	
LV Ejection fraction <50%	1.23 (0.45-3.40)	0.68	
E/A ratio (>2.3)	2.06 (0.70-6.04)	0.19	
E prime (>0.05 m/s)	0.77 (0.29-2.07)	0.61	
E/e' ratio (>16)	1.54 (0.55-4.33)	0.41	

Data is presented as hazard ratio (95% confidence interval), P value.

Study limitations

Several potential limitations of this study merit consideration. The current study was an observational study from a single center. The number of patients included in the present study was relatively small. The data may not be representative of other cohorts of patients with amyloidosis.

Conclusion

The QRS-T angle is associated with indices of advanced amyloid disease and is an independent predictor of outcome. It could be helpful in risk assessment of patients with amyloidosis.

Disclosures

None of the authors have any conflict of interests to declare.

CRediT authorship contribution statement

Anna Turyan Medvedovsky: Investigation, Writing - original draft. Arthur Pollak: Investigation. Mony Shuvy: Writing - review & editing. Israel Gotsman: Conceptualization, Writing - review & editing, Visualization, Supervision.

References

- [1] Dubrey S. The clinical features of immunoglobulin light-chain (AL) amyloidosis with heart involvement. QJM 1998;91:141–57.
- [2] Fikrle M, Paleček T, Kuchynka P, et al. Cardiac amyloidosis: a comprehensive review. Cor Vasa 2013;55:e60–75.
- [3] Falk RH, Alexander KM, Liao R, et al. AL (light-chain) cardiac amyloidosis. J Am Coll Cardiol 2016;68:1323–41.
- [4] Koyama J, Falk RH. Prognostic significance of strain Doppler imaging in light-chain amyloidosis. JACC Cardiovasc Imaging 2010;3:333–42.
- [5] Kyle RA, Linos A, Beard CM, et al. Incidence and natural history of primary systemic amyloidosis in Olmsted County, Minnesota, 1950 through 1989. Blood 1992;79: 1817–22.
- [6] Banypersad SM, Moon JC, Whelan C, et al. Updates in cardiac amyloidosis: a review. J Am Heart Assoc 2012;1:e000364-e.
- [7] Aro Al, Huikuri HV, Tikkanen JT, et al. QRS-T angle as a predictor of sudden cardiac death in a middle-aged general population. Europace 2011;14:872–6.
- [8] Pavri BB, Hillis MB, Subacius H, et al. Prognostic value and temporal behavior of the planar QRS-T angle in patients with nonischemic cardiomyopathy. Circulation 2008; 117:3181–6.
- [9] Borleffs CJ, Scherptong RW, Man SC, et al. Predicting ventricular arrhythmias in patients with ischemic heart disease: clinical application of the ECG-derived QRS-T angle. Circ Arrhythm Electrophysiol 2009;2:548–54.
- [10] Gotsman I, Keren A, Hellman Y, et al. Usefulness of electrocardiographic frontal QRS-T angle to predict increased morbidity and mortality in patients with chronic heart failure. Am J Cardiol 2013;111:1452–9.
- [11] Chen S, Hoss S, Zeniou V, et al. Electrocardiographic predictors of morbidity and mortality in patients with acute myocarditis: the importance of QRS-T angle. J Card Fail 2018:24:3–8.
- [12] Gotsman I, Shauer A, Elizur Y, et al. Temporal changes in electrocardiographic frontal QRS-T angle and survival in patients with heart failure. PLoS One 2018;13:e0194520.
- [13] Kumar S, Dispenzieri A, Lacy MQ, et al. Revised prognostic staging system for light chain amyloidosis incorporating cardiac biomarkers and serum free light chain measurements. I Clin Oncol 2012:30:989–95.